

# Magnetorheology of Multiwalled Nanotube Dispersions in Mineral Oil

Nandika Anne D'Souza<sup>+</sup> and Zhengtao Yang

Department of Materials Science and Engineering, University of North Texas

P.O. Box 305310, Denton, Texas 76203 USA

+ [ndsouza@unt.edu](mailto:ndsouza@unt.edu) (corresponding author)

Received March 23, 2007; received in revised form May 12, 2007 accepted May 16 2007

**Keywords:** Magnetorheology; multiwalled carbon nanotubes; oscillatory testing; magnetosweeps.

**Abstract.** The magnetorheological (MR) effect of multi-walled carbon nanotubes (MWNT) was investigated. Three concentrations of MWNT were dispersed in mineral oil (0.5, 1.5 and 2.53 vol% nanotubes). Rheological investigations were conducted on a magnetorheological cell coupled to a controlled stress rheometer. Oscillatory tests and rotational tests were conducted. A sinusoidal strain between 0 and 1 with a frequency of 1 Hz was applied and the stress amplitude measured for 0, 171 and 343 kA/m magnetic field strengths. Linear viscoelasticity was determined to exist at strains less than 5%. Dynamic frequency sweeps were conducted at a strain of 1% between 0 and 100 radians/s. A crossover from viscous to elastic behavior was observed for some concentrations. The crossover frequency decreased with field strength as well as with concentration of MWNT. Rotational tests were conducted between shear rates of 0 to 100/s. All dispersions had a zero shear yield stress indicative of Bingham behavior. A magnetosweep was conducted by keeping the strain within the linear viscoelastic region at a frequency of 1 Hz and ramping the magnetic field strength from 0 to 343 kA/m. The results indicate that MWNT show MR behavior.

## Introduction

Magnetorheological (MR) fluids consist of meso-scale (1-10  $\mu\text{m}$ ) ferromagnetic or ferromagnetic particles with high permeability dispersed in a viscous or viscoelastic nonmagnetizable liquid. The most common magnetic material used for the preparation of MR fluids is high purity iron powder derived from decomposition of iron penta-carbonyl ( $\text{Fe}(\text{CO})_5$ ). In the absence of an applied magnetic field, (MR) fluids typically behave as nearly ideal Newtonian liquids. The application of a magnetic field induces a magnetic dipole and multipole moments on each particle. The anisotropic magnetic forces between pairs of particles promote the head-to-tail alignment of the moments and draw the particles into proximity. These attractive interparticle forces result in the formation of chains, columns, or more complicated networks of particles aligned in the direction of the magnetic field. Magnetic flux density of the order of 0.1 Tesla can greatly increase the viscosity of MR fluids by several orders of magnitude. When these structures are deformed mechanically, magnetic restoring forces tend to oppose the deformation [1]. Their flow in an external magnetic field undergoes competition between magnetic and hydrodynamic forces. This competition gives rise to the unique rheological properties with the creation of an apparent yield stress and a rapid and reversible liquid-solid transition.

Rabinow first reported the MR effect in 1948 [2]. MR fluids can exhibit yield stress of the order of 100 kPa, two orders of magnitude larger than electrorheological (ER) fluids, when they are exposed to magnetic fields of 240 kA/m. The availability of MR fluids with yield stresses that are controllable over many orders of magnitude by applied fields enables the construction of electromechanical devices that are controlled by electrical signals. The substantial field-induced yield stresses exhibited by MR fluids have resulted in their applications in rotary brakes and linear dampers. Many ceramic, metal and alloy based compositions have been described and can be used to prepare MR fluids. Particles used are magnetically multi domain and exhibit low levels of

magnetic coercivity. Ginder [3] investigated MR fluids using numerical and analytical models and identified three regimes: at low applied fields, the yield stress increases with applied field  $H_0$  as  $\tau_y \sim H_0^{3/2}$ . In intermediate fields, the contact or polar regions of each particle saturate, reducing the rate of increase of the stress with increasing field. At high fields, the particles saturate completely, and the stress reaches its limiting value. Klingenberg [4] examined the flow modification in MR fluids associated with the field-induced magnetization of the dispersed phase relative to the continuous phase. At moderate to high particle concentration, the structure mainly consists of thick clusters. The relaxation process is related to a frequency dependent dynamic structure within the cluster.

The magnetic response of nanotubes has been of increasing interest. The graphitic nature of the nanotube lattice results in a fiber with high stiffness, strength and conductivity. Their exceptional stiffness, strength, resilience and high aspect ratio combined with their low densities offer tremendous opportunities for the development of nanotube-based composite materials. However, single wall nanotubes (SWNTs) tend to assemble in bundles (ropes) of nanotubes with weak van der Waals bonds between them and have very low solubility in most solvents. Multi-walled nanotubes (MWNTs) consist of multi-walled co-axial tubules with weak van der Waals interactions existing between coaxial graphene layers. Magnetic fields have been found to have strong effects on the electronic and bulk properties of nanotubes. Ramirez and coworkers [5] found nanotubes have significantly larger orientation-averaged susceptibility, on a per carbon basis, than any other form of elemental carbon. Lu [6] predicted a field-induced metal-insulator transition for all nanotubes. The magnetic susceptibility was predicted to be large and increase linearly with the nanotube radius. The susceptibility can be either diamagnetic or paramagnetic in a weak field depending on the field direction, the Fermi energy, the helicity of the nanotubes, and the nanotube radius.

Nanotubes have been predicted to have an anisotropic magnetic susceptibility. Wang [7] measured the magnetic susceptibility of buckybundles parallel and perpendicular to the bundle axes and found the buckytubes had anisotropic diamagnetic properties. The lowest energy orientation of nanotubes is parallel to the field so a strong magnetic field can align nanotubes in a liquid suspension, which is similar to the alignment of liquid crystal in a magnetic field. The magnetic orientation of nanotubes is explained by the susceptibility anisotropy [8]. They are magnetically symmetric along the tube axis and have molar susceptibilities parallel ( $\chi_{\parallel}$ ) and perpendicular ( $\chi_{\perp}$ ) to it. The magnetic energy of nanotubes composed of mole number  $n$  of carbon atoms in a field  $H$  is given by

$$E(\theta, H) = -(nH^2/2) [\chi_{\perp} + (\chi_{\parallel} - \chi_{\perp}) \cos 2\theta] \quad (1)$$

where  $\theta$  is the angle between the tube axis and field  $H$ . The orientation of nanotubes in a magnetic field occurs so that the energy  $E(\theta, H)$  is a minimum. Experimental observations show nanotubes are aligned with the tube axis parallel to the field ( $\theta = 0$ ). Nanotubes are considered to be diamagnetic at 310 K, that requires the condition of  $\chi_{\perp} < \chi_{\parallel} < 0$ . The field intensity dependence of the orientation of nanotubes is interpreted as the Boltzmann distribution for the directions of different magnetic energy [8]. The magnetic energy is a minimum and nanotubes are stable when the nanotube axis is parallel to the field ( $\theta = 0$ ). If the magnetic field strength is low, the difference in magnetic energy is small between the stable direction ( $\theta = 0$ ) and any direction and the orientation is disordered by the thermal energy. When the magnetic field strength increases, the difference in magnetic energy is larger and the probability of orientation in the stable direction becomes higher. Fujiwara [9] suspended MWNTs in carbon tetrachloride and placed them in magnetic fields of  $<80.0$  kOe at 310 K. They found that a single and free nanotube oriented with the tube axis parallel to the fields using SEM and estimated the anisotropy of susceptibilities parallel ( $\chi_{\parallel}$ ) and perpendicular ( $\chi_{\perp}$ ) to the tube axis to be  $\chi_{\parallel} - \chi_{\perp} \sim (9 \pm 5) \times 10^{-6}$  emu per mole of carbon atoms ( $\chi_{\perp} < \chi_{\parallel} < 0$ ). Calculations have shown that metallic SWNTs are paramagnetic in the direction of their long axes and tend to align parallel to an external magnetic field. Some SWNTs are

diamagnetic and their diamagnetic susceptibilities are most negative in the direction perpendicular to the tube axis, causing them to align parallel to the direction of an external magnetic field. The alignment energies for both magnetic and diamagnetic SWNTs are comparable. The predicted molar susceptibility for a (10, 10) nanotube are:  $\chi_{\parallel} = +85.4 \times 10^{-6} \text{ emu (molC)}^{-1}$  when parallel to B, and  $\chi_{\perp} = -21.0 \times 10^{-6} \text{ emu (molC)}^{-1}$  when perpendicular. The alignment energy is small and the effects of thermal energy should be considered. The potential energy  $U$  of a nanotube containing  $n$  moles of carbon is  $U(\theta) = -B_2 n (\chi_{\parallel} \cos 2\theta + \chi_{\perp} \sin 2\theta)$ , where  $\theta$  is the angle between the nanotube axis and the magnetic field. Each nanotube undergoes Brownian motion in this potential with an average energy of  $kBT$ , where  $T$  is room temperature. The alignment energy is  $\Delta U = U(\pi/2) - U(0) = B_2 n (\chi_{\parallel} - \chi_{\perp})$ .  $\Delta U$  must be many times  $kBT$  in order to obtain good alignment of nanotubes. For a (10, 10) nanotube of length 300 nm, a field of 15.3 T gives  $\Delta U = 5 \text{ kBT}$  [10]. The alignment energy is proportional to the number of moles of carbon. A bundle of nanotubes requires a less magnetic field to achieve alignment than an individual nanotube with the same length [10]. Walters et al. [10] produced highly aligned SWNTs in thin membranes by introducing a suspension of SWNT segments to a strong magnetic field to align the segments and filtering the suspension in the magnetic field. The obtained membranes displayed natural cleavage planes parallel to the magnetic field. Casavant et al. [11] fabricated thick macroscopic membranes of aligned SWNTs via high-pressure filtration of aqueous surfactant-suspended nanotubes using magnetic field strengths of 7 and 25 T. Their 10  $\mu\text{m}$ -thick membrane with surface areas of 125  $\text{cm}^2$  showed anisotropy of  $(2.5 \pm 0.5)$  via a polarized Raman spectroscopy. Kimura [12] prepared an anisotropic MWNT/polyester composites using a high magnetic field of 10 T and the MWNTs were found to be aligned parallel to the magnetic field inside the polymer matrix. Their results of magnetic susceptibility, electric conductivity, and elastic modulus measurements showed clear anisotropy.

The objective of this paper is to probe whether magnetic fields can induce a magnetorheological effect in multiwalled carbon nanotubes dispersions with mineral oil. We have established a response in single walled carbon nanotube dispersions [13]. Strain, frequency and shear rate effects on the dispersions are probed. Magnetosweeps are conducted to evaluate the field dependent response.

## Experimental

MWNTs were provided by Mitsui in Japan. The iron content of MWNT was determined to be 0.281 wt% using atomic absorption spectrometer. Mineral oil was purchased from Roberts Pharmaceutical Corporation. MWNTs of 1 wt%, 3 wt% and 5 wt% were dispersed in mineral oil and the corresponding volume fractions of nanotubes were determined to be 0.5, 1.5 and 2.53 vol%, respectively based on a density of  $1.75 \text{ gm/cm}^3$ . To prepare dispersions, MWNTs were added to mineral oil in a glass beaker and the mixture was stirred for about 2 minutes and heated in an oven at  $50^\circ\text{C}$  for about 3 minutes to reduce the viscosity and mixed again until the sample cooled down. The same procedure was repeated three times.

A Physica rheometer MCR 500 provided by Parr Physica was used for rheological measurements of dispersions. Applying an electric current to a coil below the bottom plate produces a magnetic field perpendicular to the parallel plates. The coil current and the magnetic field strength can be variably controlled using separate control unit and rheometer software Physica US 200 MCR. The magnetic fields strengths can be constant or applied as linear or logarithmic ramps. The software can set the magnetic field strength and perform all rheological tests available to the rheometer simultaneously. A parallel-plate measuring system with a diameter of 20 mm was used. The control unit can automatically demagnetize the system after the test is finished. The measuring system is made of non-magnetic metal to prevent the radial magnetic forces acting on the shaft of the measuring system. A two-part cover serves as magnetic bridge and gives a uniform magnetic field. The measuring system is PP 20/MR and gap selected was 0.5 mm. The required sample volume for each measurement is 0.4 cubic centimeter and a syringe of 1 cc was used to load approximate 0.4 cc

sample onto the lower plate. The sample temperature was kept at 25°C during test using a water circulator.

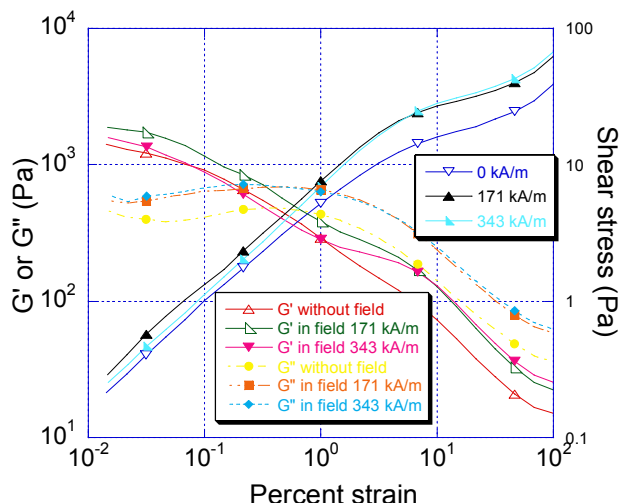


Fig. 1. Strain sweep of 2.53 vol% MWNT/mo dispersions in various magnetic field strengths at 25°C showing the  $G'$ - $G''$  crossover. The strains at  $G'$ - $G''$  crossover in magnetic field strength zero, 171kA/m and 343kA/m are 0.422%, 0.333% and 0.165% respectively, indicating the strain at  $G'$ - $G''$  crossover decreases with increasing magnetic field strength.

Oscillatory tests at low strains were carried out to avoid destroying the structure of dispersion. First, the linear viscoelastic region (LVR) was determined by the dynamic strain sweep under constant frequency in different magnetic fields. Second, dynamic frequency sweeps were conducted at constant strain within (LVR) in different magnetic fields to investigate the structure of the dispersions. In these sweeps, the strain was kept constant at 1% and the angular frequency  $\omega$  ramped logarithmically from 100 to 1 (1/s) with 6 data points collected in each decade.  $G'$ ,  $G''$  and  $\eta^*$  were measured. Third, steady shear tests were conducted to investigate the flow behavior materials and flow curves were obtained under a controlled shear rate (CSR) in different magnetic fields. The shear rate ramped logarithmically from 10 to 200 (1/s) for MWNT/mo with 6 data points collected in each decade. Shear stress  $\sigma$  and viscosity  $\eta$  were recorded at logarithmically varied shear rate.

## Results

**Oscillatory Tests.** The strain sweep results for 0.5, 1.5 and 2.53 vol.% MWNT/mo are shown in Fig 1. Storage modulus results corresponding to a strain of 1% are tabulated in Table 1. For low concentrations 0.5 and 1.5vol%, increasing the field strength increased  $G'$  and  $G''$  in a sample. The increase was roughly linear. The results indicate that alignment of the tubes perpendicular to the plates leads to increases in complex shear moduli. However, at higher nanotube concentration, (2.53 vol%),  $G'$  first increases and then decreases. A  $G'$ - $G''$  crossover implying a solid-liquid transition was evident in the relatively high concentration 1.5 and 2.53 vol% sample. The solid-liquid transition is reflective of the presence of a flocculated network. The strain at  $G'$  - $G''$  crossover is defined as the critical strain is listed in Table 2 for MWNT/mo dispersion. The critical strain decreased with field strength. This indicates that as the field strength increases, the solid-liquid transition occurs at lower strains. The yield stress increased with magnetic field strength for all

compositions. Increased concentration of MWNT’s had a substantial effect in increasing the yield stress for a given field strength.

Table 1. The storage modulus  $G'$  at strain of 1% for strain sweep of MWNT/mo dispersions.

Magnetic field strength (kA/m)	0	171	343
Magnetic flux density (Tesla)	0	0.215	0.431
$G'$ (0.5 vol%MWNT/mo) (Pa)	5.8	7.1	8.5
$G'$ (1.5 vol%MWNT/mo) (Pa)	40.8	49.5	58.6
$G'$ (2.53 vol%MWNT/mo) (Pa)	290	384	283

Table 2. Critical strain corresponding to  $G'$ - $G''$  crossover and yield stress for MWNT/mo dispersions in various magnetic fields.

Sample	Magnetic field strength (kA/m)	Magnetic flux density (Tesla)	Critical strain $\gamma_c$	Yield stress (Pa)
0.5 vol%MWNT/mo	0	0	-	1.9
0.5 vol%MWNT/mo	171	0.215	-	2.0
0.5 vol%MWNT/mo	343	0.431	-	2.24
1.5 vol%MWNT/mo	0	0	1.64%	5.6
1.5 vol%MWNT/mo	171	0.215	0.61%	5.9
1.5 vol%MWNT/mo	343	0.431	1.26%	8.2
2.53 vol%MWNT/mo	0	0	0.42%	89.3
2.53 vol%MWNT/mo	171	0.215	0.33%	103.1
2.53 vol%MWNT/mo	343	0.431	0.17%	130.3

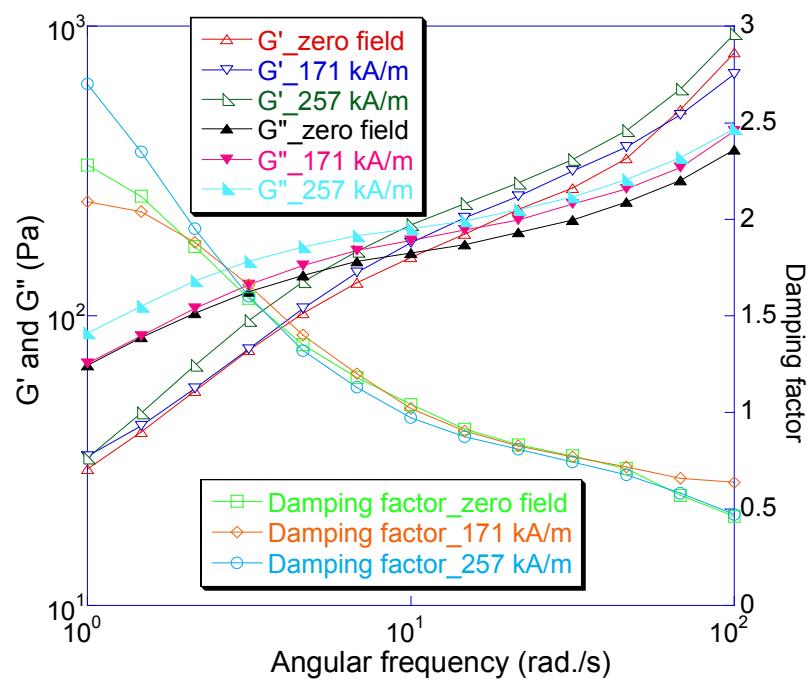


Fig. 2 Frequency sweep for 1.5 vol% MWNT/mo dispersions in various magnetic field strengths at 25° C.

Fig 2. shows the results of the dynamic frequency sweeps.  $G'$  and  $G''$  are a function of frequency and increases with increase frequency and the behavior was concentration dependent. At 0.5 vol% MWNT/mo, the magnetic field has a very weak effect on  $G'$  and  $G''$  and the two curves are almost identical. At 1.5 vol% MWNT/mo, both  $G'$  and  $G''$  increase with magnetic field. At 2.53vol%  $G'$  and  $G''$  first increase then decrease with magnetic field which is consistent with the strain sweep results for 2.53vol% in Table 1. We examine the frequency dependence. For entangled polymer solutions and melts, we know that  $G'$  is proportional to  $\omega^2$  and  $G''$  is proportional to  $\omega$ . In the absence of a field, at low concentrations (up to 1.5 vol%), the values mimic that of entangled polymer solutions. However, at a higher concentration such as 2.53 vol% a deviation from the proportionality is evident with  $G'$  and  $G''$  having a weak dependence on frequency, especially in low frequency region. At high concentrations, there is therefore evidence that the MWNT/mo dispersion behaves like a gel. This phenomenon has been evident in aqueous nanotube dispersions studied by Kinloch et al. [14]. We also note a solid-liquid transition by examining the  $G'$ - $G''$  crossover as a function of frequency listed in Table 3. We note the absence of a crossover at high MWNT concentrations. In the absence of a field, the crossover frequency decreases with increasing nanotube concentration. As the field strength increases, the crossover frequency decreases with increasing field strength, but the magnitude of the change was marginal.

Table 3. Angular frequency  $\omega$  (rad/s) at  $G'$ - $G''$  crossover for mineral oil and MWCNT/mo dispersions in different magnetic fields.

Magnetic field strength (kA/m)	0	171	257	343
Magnetic flux density (Tesla)	0	0.215	0.323	0.431
mineral oil (rad/s)	14.9	22.8	19.6	-
0.5 vol%MWCNT/mo	28.18	-	-	24.48
1.5 vol%MWCNT/mo	11.36	10.58	9.38	10

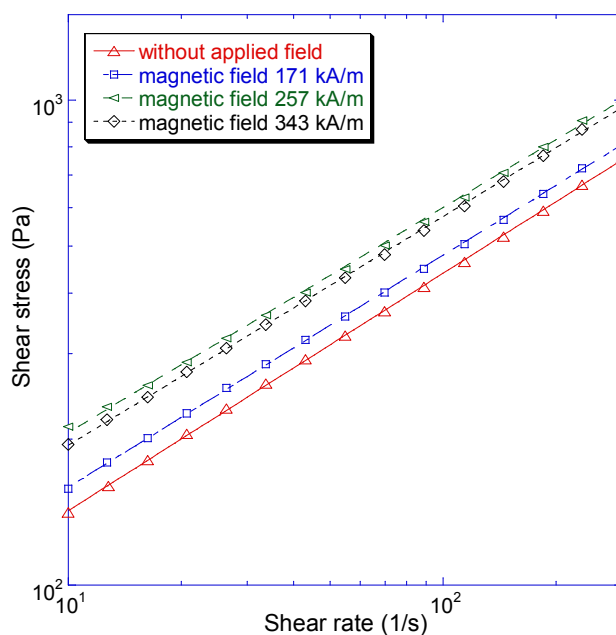


Fig.3 Flow curves of 2.53 vol% MWNT/mo dispersion in various magnetic field strengths at 25°C.

$G'$  and  $G''$  increase with increasing nanotube volume fraction,  $\phi$ . The  $G'$  and  $G''$  measured at the frequency of 1 (rad/s) extracted from frequency sweep data are fitted to a power law. Power law relationship between  $G$  and  $\phi$  has been found theoretically and experimentally for flocculated systems. The experimental values of 2.4 to 4.4 for the power law index have been reported [17]. The relationships for the data are given by:

$$G' = 19.496\phi^{3.63} \text{ with fit quality } R=0.99$$

$$G'' = 29.48\phi^{2.93} \text{ with fit quality } R=0.99$$

**Rotational Tests.** Steady shear properties were analyzed from the flow curves of the dispersions. Fig. 3 shows typical flow curves of MWCNT/mo dispersions. The shear stress increases with increasing shear rate and also increases slightly with increasing magnetic field strength at the same shear rate for nanotube concentrations up to 1.5vol%. At a concentration of 2.53vol%, a more pronounced increase in shear stress with increasing magnetic field at the same shear rate is observed. Following the Bingham model, the yield stress was obtained by extrapolating the shear stress-shear rate data to zero shear rate and finding the intersection with the vertical axis and the results are presented in Table 4.

Table 4 Yield stress for MWCNT/mo dispersions in various magnetic fields.

Sample	Magnetic field strength (kA/m)	Magnetic flux density(Tesla)	Yield stress (Pa)
0.5 vol%MWCNT/mo	0	0	1.9
0.5 vol%MWCNT/mo	171	0.215	1.982
0.5 vol%MWCNT/mo	343	0.431	2.238
1.5 vol%MWCNT/mo	0	0	5.58
1.5 vol%MWCNT/mo	171	0.215	5.95
1.5 vol%MWCNT/mo	343	0.431	8.21
2.53 vol%MWCNT/mo	0	0	89.29
2.53 vol%MWCNT/mo	171	0.215	103.13
2.53 vol%MWCNT/mo	257	0.323	146.55
2.53 vol%MWCNT/mo	343	0.431	130.33

The yield stress increases greatly with rising concentration and also increases with increasing magnetic field at the same concentration. The yield stresses for different magnetic flux densities are fitted to the power using the following relationships:

$$\tau_y \sim 2.59B^{0.17} \text{ for 0.5vol\%MWCNT/mo dispersion}$$

$$\tau_y \sim 12.1B^{0.46} \text{ for 1.5vol\%MWCNT/mo dispersion}$$

$$\tau_y \sim 388.8B^{0.86} \text{ for 2.53vol\%MWCNT/mo dispersion}$$

For iron-based magnetorheological (MR) fluids carbonyl iron particles in poly (dimethyl siloxane) or silicone oil (for  $\phi=0.4$ ),  $\tau_y \sim B^{1.5}$  relationship has been observed [1] Phule and Ginder observed Bingham plastic behavior for both iron-based and ferrite-based MR fluids and found that yield stress increased as  $B^{1.5}$  at an applied magnetic flux density below 1 Tesla, which is a consequence of the local saturation of the magnetization in the polar or contact zones of each particles [14]. In the MWNT/mo dispersions, both the coefficients and indices for the yield stress increase dramatically with increasing concentration.

Non-Newtonian flows are often described by the Ostwald-de Waele or so-called power law model:

$$\tau = k\dot{\gamma}^n \quad (2)$$

$$\eta = k\dot{\gamma}^{(n-1)} \quad (3)$$

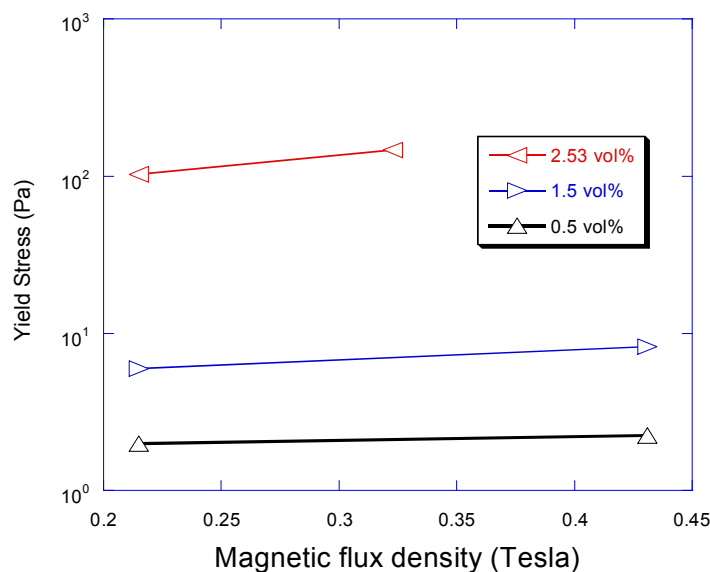


Fig. 4 Yield stress versus magnetic flux density for MWCNT/mo dispersion. The open triangles represent measured yield stresses which are fitted to power law.

where the constant  $k$  is the consistency index and represent the viscosity for a Newtonian fluid. The constant  $n$  is the flow index, which indicates the degree of deviation from Newtonian behavior ( $n=1$ ). The values of consistency index  $k$  and flow index  $n$  for MWNT/mo dispersions are presented in Table 5. We can see all power law indices of MWNT/mo dispersions in various magnetic fields are less than 1; therefore, all systems are pseudoplastics, which display shear thinning. Furthermore, increasing magnetic field slightly decreases the  $n$  and increases the  $k$ . For instance,  $n$  decreases from 0.489 to 0.472 and  $k$  increases from 46.14 to 65.45 when the applied magnetic field strength increases from 0 to 343 kA/m for 2.53vol%MWNT/mo dispersion. In the same magnetic field, increasing nanotube concentration increases the  $k$  values but decreases the  $n$  values.

Table 5. Consistency index ( $k$ ) and flow index ( $n$ ) obtained from steady shear tests for MWNT/mo dispersions in various magnetic fields.

Magnetic field strength (kA/m)	0	171	343
Magnetic flux density (Tesla)	0	0.215	0.431
$k$ ( 0.5 vol% MWNT/mo)	1.052	1.01	1.17
$k$ ( 1.5 vol% MWNT/mo)	2.4	2.47	3.15
$k$ ( 2.53 vol% MWNT/mo)	46.14	52.81	65.45
$n$ ( 0.5 vol% MWNT/mo)	0.866	0.868	0.854
$n$ ( 1.5 vol% MWNT/mo)	0.75	0.748	0.726
$n$ ( 2.53 vol% MWNT/mo)	0.489	0.479	0.472

**Magnetosweep Results.** The magnetosweep data for all concentrations at constant frequency and constant shear rate are shown in Fig 5. The  $G'$ ,  $G''$ , and  $\eta^*$  increase marginally with rising magnetic field strength. The  $G'$ ,  $G''$  and  $\eta^*$  during magneto sweep are normalized or divided by those corresponding values measured at the beginning of the magneto sweep test with a zero applied field. The lowest nanotube concentration 0.5vol% exhibits the largest percent increase in  $G'$ ,  $G''$  and  $\eta^*$  when the magnetic field increases linearly from zero to 343 kA/m while the highest nanotube concentration 2.53vol% displays the lowest relative increase in  $G''$  and  $\eta^*$ . This is due to the fact



that increasing nanotube loading in mineral oil results in a dramatic increase in the viscosity of the dispersion and the increasing difficulty with which nanotubes can be aligned. At 2.53 vol%, flocculated system is formed where nanotubes closely touch each other and rotation of nanotubes along the field direction is hindered. The highest nanotubes concentration, 2.53vol%MWCNT/mo, exhibits the smallest relative increase in  $G'$ ,  $G''$  and  $\eta^*$  when the magnetic field strength is linearly increased because nanotubes have difficulty in being aligned in both viscous dispersions behaving like a gel. Both results indicate that it is the alignment of nanotubes by the magnetic field, not the iron content, that causes the observed increase in  $G'$ ,  $G''$  and  $\eta^*$ .

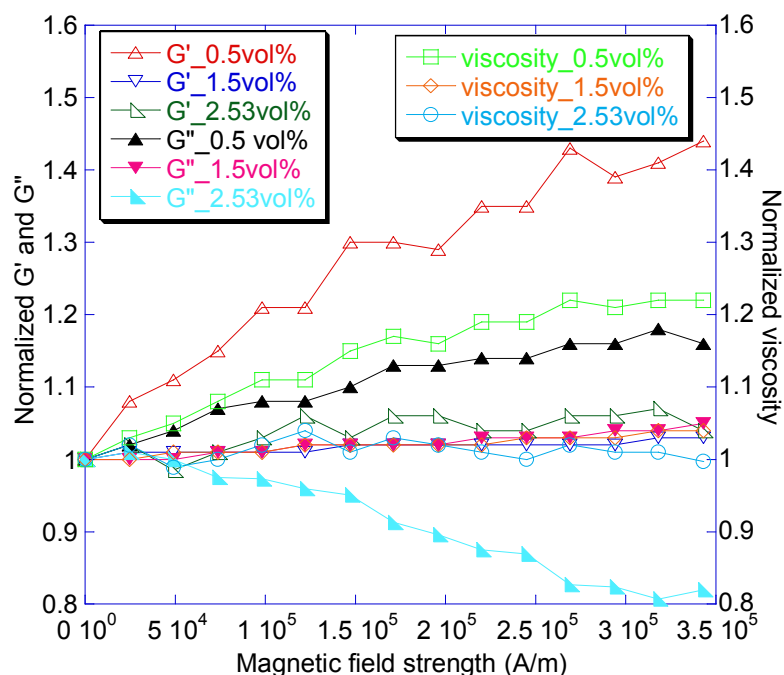


Fig. 5 Normalized (to the values for field=0)  $G'$ ,  $G''$ ,  $\eta^*$  for MWCNT/mo dispersions using magneto sweep data at 25° C.

## Summary

Residual iron and intrinsic response of multi-walled carbon nanotubes results in a magnetorheological behavior in mineral oil. Oscillatory shear tests showed a crossover from viscous to elastic response with increasing field strength. The crossover was further examined by dynamic frequency sweeps at a constant strain amplitude. The crossover persisted indicating a flocculated network of entangled nanoparticles. Flow curves indicated a Bingham fluid which had a field strength dependence. Magnetosweeps indicated that lower concentrations were more effective in contributing the MR response.

## Acknowledgements

We thank Gina Paroline of Paar Physica for excellent technical support.

## References

- [1] J.M. Ginder, Behavior of magnetorheological fluids. MRS Bulletin August 1998, 26-29.
- [2] J. Rabinow, The Magnetic Fluid Clutch, AIEE Trans 67 (1948) 1308.

- 
- [3] J. M. Ginder, L. C. Davis, L. D. Elie, Rheology of magnetorheological fluids: models and measurement, *Intern. J. Modern Physics B* 10 (1996) 3293-3303.
  - [4] D. J. Klingenberg, Simulation of the Dynamic Response of Electrorheological Suspensions: Demonstration of a Relaxation Mechanism, *J. Rheology* 37 (1993) 199-214.
  - [5] A. P. Ramirez, R. C. Haddon, O. Zhou, R. M. Fleming, J. Zhang, S. M. McClure, R. E. Smalley, Magnetic Susceptibility of Molecular Carbon: Nanotubes and Fullerite, *Science* 265 (1994) 84-86.
  - [6] J. P. Lu, Novel Magnetic Properties of Carbon Nanotubes, Growth and characterization of buckybundles *Phys. Rev. Lett.* 74 (1995) 1123-1126.
  - [7] X. Wang, X. W. Lin, V. P. Dravid, J. B. Ketterson, R. P. H. Chang, *Appl. Phys. Lett.* 62 (1993) 1881- 883.
  - [8] M. Fujiwara, M. Fukui and Y. Tanimoto, Magnetic Orientation of Benzophenone Crystals in Fields up to 80.0 KOe, *J. Phys. Chem. B* 103 (1999) 2627-2630.
  - [9] M. Fujiwara, E. Oki, M. Hamada, Y. Tanimoto, I. Mukouda, Y. Shimomura, Magnetic Orientation and Magnetic Properties of a Single Carbon Nanotube, *J. Phys. Chem. A* 105 (2001) 4383-4386.
  - [10] D.A. Walters, M.J. Casavant, X.C. Qin, C.B. Huffman, P.J. Boul, L.M. Ericson, E.H. Haroz, M.J. O'Connell, K. Smith, D.T. Colbert, R.E. Smalley, In plane aligned membranes of carbon nanotubes, *Chem. Phys. Lett.* 338 (2001) 14-20.
  - [11] M.J. Casavant, D.A. Walters, J.J. Schmidt, R.E. Smalley, Neat macroscopic membranes of carbon nanotubes, *J. Appl. Phys.* 94 (2003) 2153-2156.
  - [12] T. Kimura, H. Ago, M. Tobita, S. Ohshima, M. Kyotani and M. Yumura, Polymer Composites of Carbon Nanotubes Aligned by a Magnetic Field, *Advanced Mater.* 14 (2002) 1380-1383.
  - [13] Z. Yang, J. Bahr and N. A. D'Souza, Magnetorheology of single wall carbon nanotubes in mineral oil, *J. Intell. Mater. Smart Struct.*, submitted.
  - [14] P.P. Phule, J M Ginder, Synthesis and Properties of Novel Magnetorheological Fluids Having Improved Stability and Redispersibility, *Intern. J. Modern Physics B* 13 (1999) 2019-2027.